# Structure of Metallic Glasses: Experiments and Models

P. Lamparter and S. Steeb

Max-Planck-Institut für Metallforschung, Institut für Werkstoffwissenschaft, Seestraße 92, D-70174 Stuttgart

Z. Naturforsch. **51a**, 983–990 (1996); received June 3, 1996

The topological and the chemical short range order in metallic glasses is discussed by means of representative examples from the systems Ni-P, Ni-B, Nb-Ni, and Dy-Ni. The characterization of the chemical short range order, e.g. in terms of a short range order parameter, depends on the definition of an appropriate hypothetic statistical reference system. The consideration of the size effect is essential. Some structural features of metallic glasses point to relationships with the related individual crystalline phases, whereas other features show that the different types of metallic glasses have certain construction principles in common. Small angle scattering with hydrogenated metallic glasses suggests the presence of extended two-dimensional structures. Reverse Monte Carlo models reveal rather broad distributions of the local structural properties and show that metallic glasses are not built as assemblies of defined structural units.

## 1. Introduction

Reliable partial pair correlation functions have been determined for a variety of metallic glasses, particularly by neutron diffraction in combination with the isotopic substitution technique. The structural parameters are well established as far as a structural description in terms of one-dimensional distribution functions and statistical averages is concerned. However, the three-dimensional arrangement of the atoms in these materials is still a subject of discussion.

In the last years there has been a shift of the activities devoted to the structure of metallic glasses from the experimental field to the field of model calculations. In fact, a state seems to be reached, where from the addition of more diffraction data to the bulk of the existent data further fundamental progress is hardly to be expected. Structural models provide access to the three-dimensional distribution of the atoms, such as bond angles and the existence of specific coordination polyhedra, as well as to the variation of local structural properties from site to site.

In the present paper a brief summary of the structural properties of metallic glasses is given. Representative examples, where reliable partial pair correlation functions have been established, are selected from the three groups: Transition metal – metalloid glasses ($Ni_{80}P_{20}$ [1] and $Ni_{81}B_{19}$ [2]), transition metal glasses ($Nb_{100-x}Ni_x$ [3]), and transition metal – rare earth metal glasses ($Dy_{44}Ni_{56}$ [4]). Since compilations of the structural data of metallic glasses, as obtained from diffraction, were already reported in previous reviews [5–7], we concentrate in the present paper on structural properties beyond pair correlations, which can be explored by model calculations.

Reprint requests to Dr. P. Lamparter.

## 2. Results from Diffraction Experiments

### *2.1 Wide Angle Diffraction*

The experimental partial pair correlation functions $G_{ij}(R)$ of the glasses discussed in the present work are shown in Figs. 1–3, where

$$G_{ij}(R) = 4\pi R\,[\varrho_{ij}(R)/c_j - \varrho_0]\,, \tag{1}$$

and

$\varrho_{ij}(R)$ = number density of $j$-atoms at distance $R$ from an $i$-atom,

$\varrho_0$ = average number density.

Several structural features are common to the different groups of metallic glasses:

i) A chemical short range order effect: The chemical interaction between the constituents causes preferred hetero-coordination in the glasses. The Cargill-Spaepen short range order parameters [8] point to stronger ordering effects in metal-metalloid glasses than in metal-metal glasses.

ii) The correlation between unlike atoms is well defined: Often the bond length distribution between unlike atoms is sharper than that between like

0932-0784 / 96 / 0900-0983 $ 06.00 © – Verlag der Zeitschrift für Naturforschung, D-72072 Tübingen

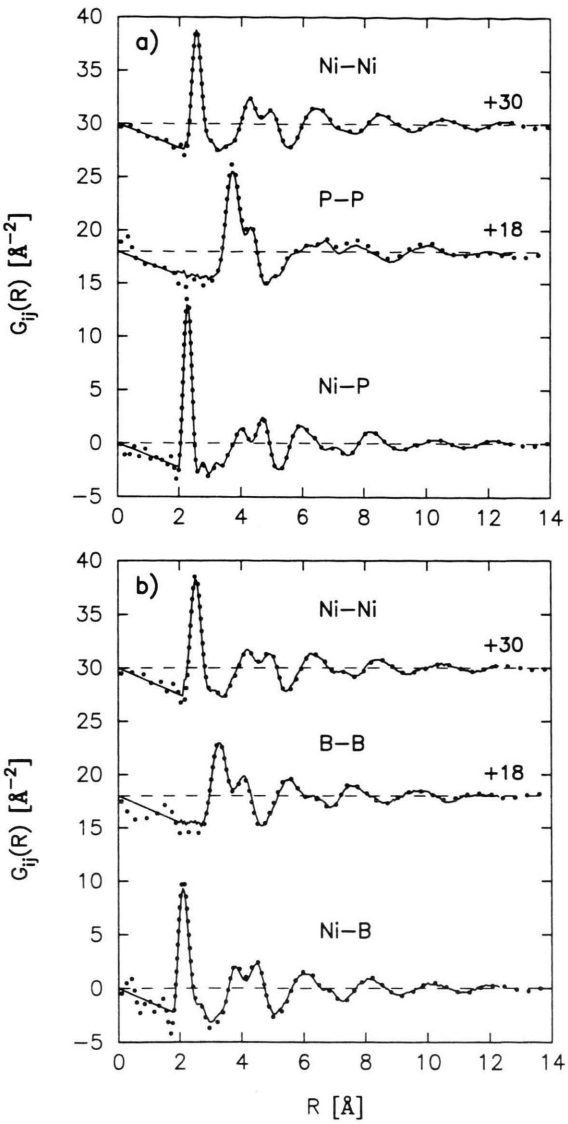


Fig. 1. a) $Ni_{80}P_{20}$, b) $Ni_{81}B_{19}$: partial pair correlation functions. ● ● ● experimental; —— Reverse Monte Carlo (RMC).

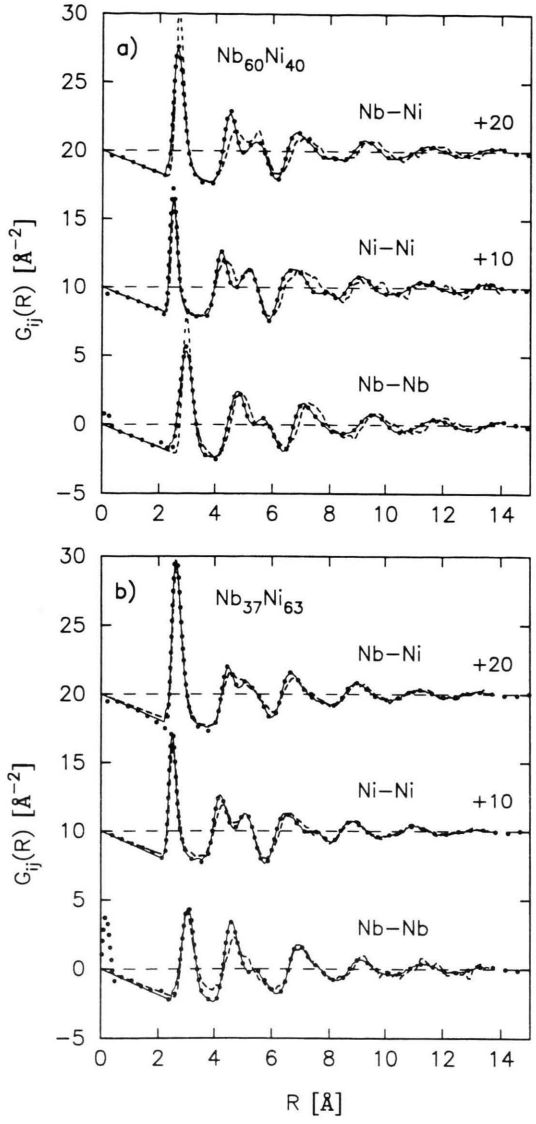


Fig. 2. a) $Nb_{60}Ni_{40}$, b) $Nb_{37}Ni_{63}$: partial pair correlation functions. ● ● ● experimental; —— Reverse Monte Carlo (RCM); – – – Cluster Relaxation (CR).

atoms, and the first and second coordination shells are well separated by a minimum in the pair distribution function, where $\varrho_{ij}(R)$ is close to zero.

iii) A contraction of the distance between unlike atoms of the order of several percent, compared to the average of the distances between like atoms. The pair potentials are non-additive. The distances between like atoms are close to their Goldschmidt diameters.

iv) A marked size effect, due to the different diameters of the constituents in glass forming alloys.

v) An asymmetric behaviour of the short range order with respect to the two constituents: The preferred hetero-coordination implies a reduction of the nearest neighbour peaks in $G_{ij}(R)$ for like atomic pairs in favour of the peak for unlike pairs. This lowering of the nearest neighbour peak is distinctly stronger for the smaller constituent (P and B in the

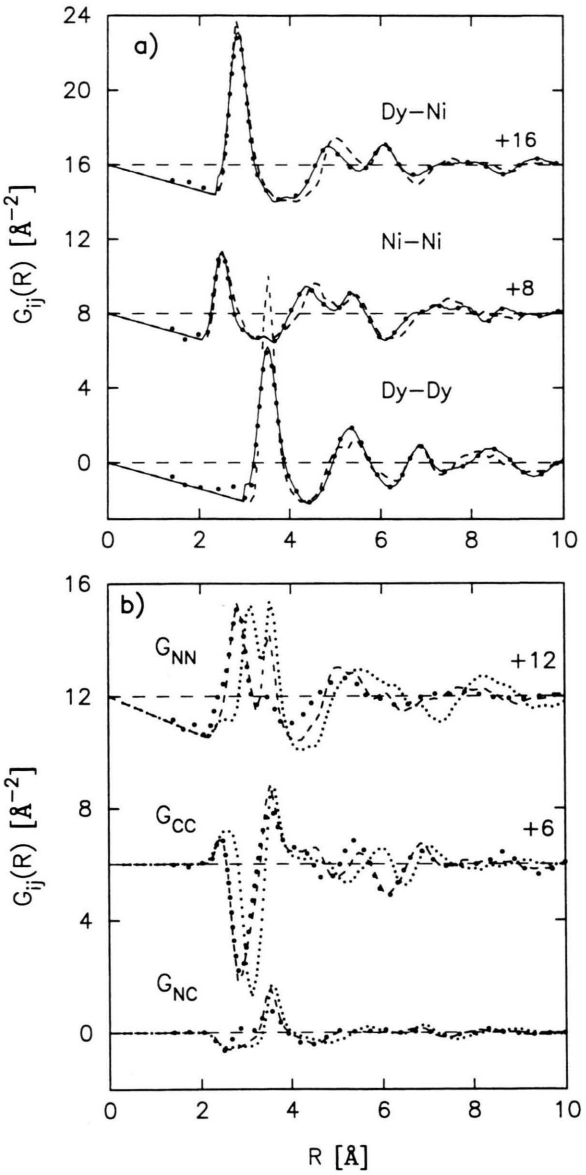


Fig. 3. $Dy_{44}Ni_{56}$: a) partial pair correlation functions. ● ● ● experimental; ——RMC; – – – CR with chemical short range order. b) Bhatia-Thornton correlation functions. ● ● ● experimental; – – – CR with chemical short range order; · · · · CR without chemical short range order (statistical reference system).

metal-metalloid glasses, and Ni in the metal-metal glasses). In $Ni_{80}P_{20}$ and $Ni_{81}B_{19}$ no direct metalloid neighbours at all were detected by experiment.

A study of the atomic structure of an amorphous alloy usually comprises a search for ordering phenomena on the basis of the diffraction data, and different approaches have been tried in such studies.

For the characterization of the short range order and a comparison of different metallic glasses it would be revealing to put a given glass on a scale ranging from no order, i.e. a statistically random distribution, up to maximum order, i.e. maximum heterocoordination. However, the definitions of the hypothetic reference systems at the end points of this scale are not unequivocal, particularly because of the size effect.

The definition of a chemical short range order parameter (see e.g. [5, 6] for compilations) is performed by comparing the coordination numbers of a glass with the corresponding ones of the statistical and the maximum ordered system, respectively. Its application is based on the assumption that the total coordination numbers around the two atomic species are the same in the real glass and in the reference systems, i.e., that they are not affected by a redistribution of the atoms. This assumption implies that the topological order is independent from the chemical order. However, this is not the case in real glasses, and the significance of a short range order parameter, as a quantitative measure, becomes rather questionable.

The distinction between topological and chemical short range order in terms of the Bhatia-Thornton correlation functions [9] is quite illuminating in case of alloys with moderate size effect.

Another approach in the search for some order in the structure of the disordered metallic glasses has been frequently tried by comparison with the structure of related crystalline phases. The motivation for this approach seems to be based on the wish to establish an illustrative picture of the three-dimensional arrangement of the atoms rather than on physical reasons that a close structural relationship between the two different states of matter is to be expected. The agreement of atomic distances, usually close to the Goldschmidt diameters, presents no crucial criterion. The agreement of coordination numbers, if found at all, is confined usually to one of the constituents. The most stringent criterion is the spatial distribution of the atoms, which however requires information about higher order correlations, such as bond angle distributions or specific coordination polyhedra. As these informations are not provided directly by the one-dimensional pair correlation functions, the construction of three-dimensional structural models is essential.

### 2.2 Small Angle Scattering

Small angle neutron scattering (SANS) experiments give evidence that many metallic glasses are not homogeneous, but contain structural fluctuations, which often occur on two different length scales (see e.g. review [10]).

Frequently a Guinier scattering law was observed in the small angle regime at scattering vectors $Q > 0.1$ Å$^{-1}$, corresponding to extensions of the scattering regions in the order of some tens of Ångstrom units. These have been ascribed to a tendency for phase separation into two different amorphous phases, e.g. the development of metalloid-enriched regions in metal-metalloid glasses.

In a second scattering regime at $Q < 0.1$ Å$^{-1}$ down to at least $10^{-3}$ Å$^{-1}$, often a power law scattering $I(Q) = \text{const} \cdot Q^{-S}$ was found with exponents $-S$ between $-3$ and $-4$, which is associated with very extended fluctuations on length scales up to at least $10^3$ Å. This phenomenon is much less understood up to now, and difficult to study because of the scattering contributions from the outer surfaces of the usually thin amorphous foils. In [11] a SANS investigation with melt-spun (Cu, Ni)-Ti-Si glasses was performed with the aim to obtain information about these extended inhomogeneities by loading the glasses with hydrogen and deuterium, respectively. Figure 4 shows the SANS cross sections for two glasses in the melt-spun state and after H(D) absorption. The power law scattering was attributed to extended inner surfaces, probably with fractal properties. The H(D) atoms tend to segregate at these inner surfaces, giving rise to an increase in the scattering contrast, which is stronger for D than for H because of its larger scattering length. The dependence of the enhancement factor on the H(D) content in Fig. 5 supports this view: At relatively low contents the enrichment at the inner surfaces is large compared with the bulk, yielding a strong contrast. With increasing content, the surfaces become saturated, and absorption of further H(D) atoms, only in the bulk, reduces the contrast again. The physical nature of these extended fluctuations, presenting most probably an inherent structural feature of metallic glasses in general, needs further exploration.

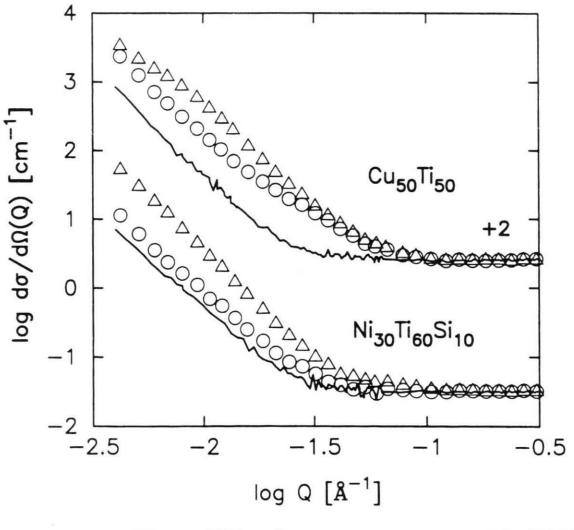


Fig. 4. $Cu_{50}Ti_{50}$ and $Ni_{30}Ti_{60}Si_{10}$: log-log plot of the SANS cross section. —— as-quenched; o loaded with 15 at% H; △ loaded with 15 at% D.

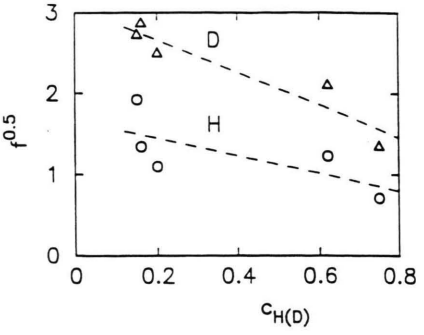


Fig. 5. Square root of the enhancement factor $f_{H(D)}$ of the SANS after H(D) loading versus the H(D) content $c_{H(D)}$. o with H; △ with D; – – – least squares fit.

## 3. Structural Models

In this section we report on investigations, where topological ordering phenomena are addressed on the basis of model clusters. In all cases the clusters were created by using a Cluster Relaxation (CR) algorithm [12] in a static mode, i.e. without velocities, and a subsequent refinement procedure by means of the Reverse Monte Carlo (RMC) method [13].

### 3.1 $Ni_{80}P_{20}$ and $Ni_{81}B_{19}$

In [14, 15] the structure of the metallic glasses $Ni_{80}P_{20}$ and $Ni_{81}B_{19}$ was simulated by RMC (Figs. 1 a, b), and the model clusters were analyzed in terms

of trigonal prisms as coordination polyhedra of the metalloid atoms. The average coordination number of about 9 Ni atoms around the metalloid atoms in the metallic glasses points to some correspondence with the related crystalline phases $Ni_3P$ and $Ni_3B$, where 9 Ni atoms form face capped trigonal prisms around the metalloid atoms, and it has been suggested that such prisms exist also in the amorphous state as favoured structural units [16, 17]. However, the analysis of the model clusters did not support the view of a stereochemical prismatic ordering, but rather gave evidence that the spatial arrangement of the Ni atoms around the metalloid atoms is a statistical one. Figures 6a, b (full symbols) show the histograms of the rotation angle $\omega$ between a triplet of 3 Ni atoms, neighbouring a metalloid atom, and a triplet of 3 further Ni atoms placed at the opposite side. A perfect trigonal prism would be characterized by $\omega = 0$. In fact, the increase towards small rotation angles indicates a certain preference for a prismatic arrangement of the 6 Ni atoms around P and B, respectively, in the RMC cluster. However, as this does not exceed substantially the preference as recorded from clusters where the Ni atoms were distributed randomly around the metalloid atoms (open symbols), we do not need any chemistry for the explanation of this behaviour. Furthermore, the fact that the stronger increase for $Ni_{81}B_{19}$ than for $Ni_{80}P_{20}$ is also found in the case of the random distributions shows that it is rather a size effect than a chemical ordering effect.

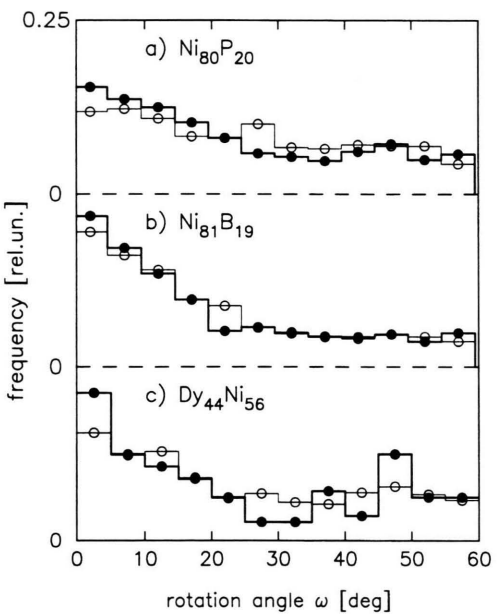


Fig. 6. Amorphous A-B alloys: histograms of rotation angle $\omega$ (see text). Full symbols from RMC model; open symbols for a random arrangement of larger atoms (A) around smaller atoms (B).

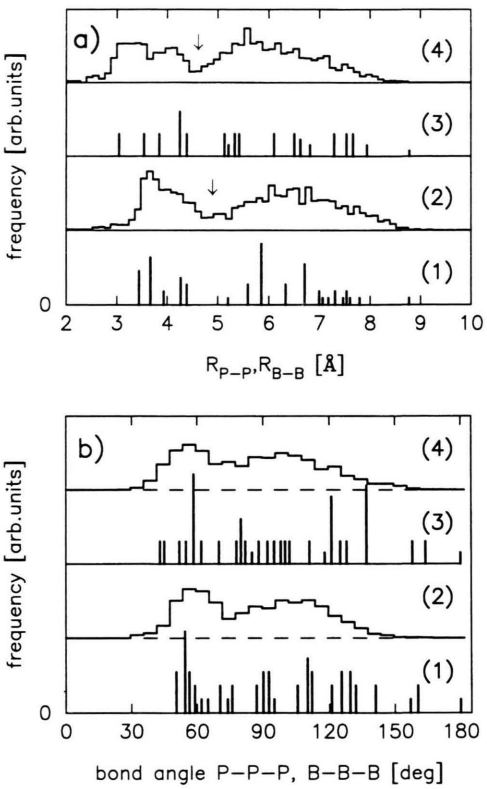


Fig. 7. Correlations between metalloid atoms which belong to the same coordination shell around a common metalloid atom. a) Distances between metalloid atoms, b) bond angles in triplets of metalloid atoms: (1) crystalline $Ni_3P$; (2) $Ni_{80}P_{20}$ (RMC); (3) crystalline $Ni_3B$; (4) $Ni_{81}B_{19}$ (RMC).

The correlation functions $G_{PP}(R)$ and $G_{BB}(R)$ in Figs. 1a, b show that besides the common structural features of transition metal–metalloid glasses there are also differences in detail, giving rise to the question of the topological arrangement of the metalloid atoms. Figure 7a displays the histograms of the distances between those metalloid atoms which belong to the same split coordination shell around a common central metalloid atom. Figure 7b shows the bond angle distributions in triplets of these atoms, taking into account neighbours up to the minimum in the distance distribution (marked by arrow in Figure 7a). No significant differences in the spatial distributions

of the P atoms and the B atoms are observed in Figs. 7a and b, apart from the somewhat sharper distance distribution for the P atoms (curve (2) in Fig. 7a) than for the B atoms (curve (4)).

The bars in Figs. 7a, b are for the crystalline phases $Ni_3P$ and $Ni_3B$. We do not observe obvious correspondence to the amorphous phases.

### 3.2 *Nb-Ni*

In an experimental investigation of the concentration dependence of the structure of amorphous $Nb_{100-x}Ni_x$ alloys ($x = 40$, 50, 56, and 63) [3] an increase of the chemical short range order with increasing Ni content was found. The structure of the glasses was simulated in a combined CR and RMC study [18]. Non-additive potentials yielded the best CR fit with rather weak preference for Nb-Ni pairs, increasing with the Ni content. Interestingly, for the $Nb_{60}Ni_{40}$ alloy no preference for Nb-Ni pairs at all had to be chosen in the potentials, in order to represent reasonably well the height of the first peak in the $G_{NiNi}(R)$ function.

The experimental result, that the partial coordination numbers around the Ni atoms extrapolated well to the values of crystalline $NbNi_3$ [3], stimulated an investigation of the topological arrangement of the Nb and Ni atoms around the Ni atoms [18]. It turned out that the similarity between the amorphous state and the crystalline state is confined to the distances and Ni-coordination numbers, but does not extend to the shape of the coordination polyhedra. Figure 8b shows the bond angle distributions in Nb-Ni-Nb triplets. The two peaks near 60° and 120° are observed in general with metallic glasses and thus give no evidence for specific atomic arrangements deviating from a dense tetrahedral packing of spheres. No significant trend is observed, such as the occurrence of additional bond angles, when increasing the Ni content, i.e. when approaching the composition of $NbNi_3$. The increasing chemical short range order does not promote specific stereochemical arrangements of the atoms. Moreover, the bond angles near 90°, which are characteristic for crystalline $NbNi_3$, are not favoured in the amorphous state.

In Fig. 8 also the distributions of the bond angle in Ni-B-Ni triplets in $Ni_{81}B_{19}$ and in Dy-Ni-Dy triplets in $Dy_{44}Ni_{56}$, as obtained from the RMC clusters, are shown as an example, out of many others, that the metallic glasses from different groups have quite similar general features. Note, that in the metal-metal glasses Ni is the smaller species, whereas in the metal-metalloid glasses Ni is the larger one. Furthermore, we note that the differences between the corresponding distributions of the crystalline phases in Fig. 8 do not appear in the amorphous alloys.

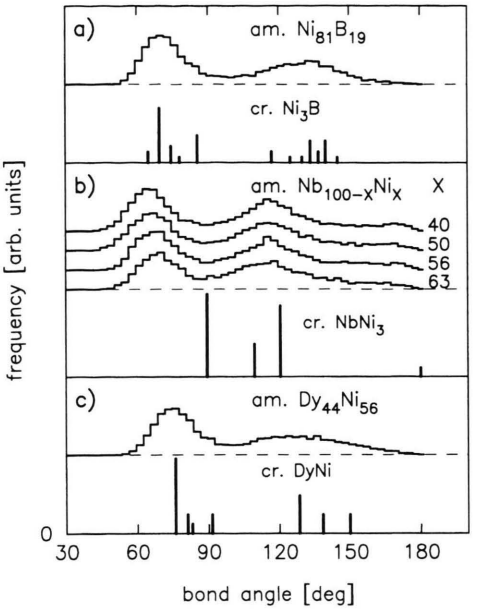


Fig. 8. Amorphous and crystalline A-B alloys: bond angles in A-B-A triplets.

### 3.3 *$Dy_{44}Ni_{56}$*

In amorphous $Dy_{44}Ni_{56}$ the average coordination number $Z_{NiDy}$ is about 6 [4]. In the crystalline phase DyNi 6 Dy atoms, out of the 7 Dy atoms around Ni, form a distorted trigonal prism, and the question arises whether this prismatic unit is found also in the glassy state. The histogram of the rotation angle $\omega$ between two opposite Dy triplets around a central Ni atom in Fig. 6c (full symbols), as calculated from a RMC cluster [19], shows a preference for small values of $\omega$, i.e. a certain degree of prismatic ordering of the Dy atoms. However, as this behaviour was found again for a random distribution of the Dy atoms around Ni (open symbols), it should not be assigned to a stereochemical ordering effect.

The distribution of the bond angle in triplets of Dy atoms which belong to the same coordination shell around a central Ni atom was calculated from the

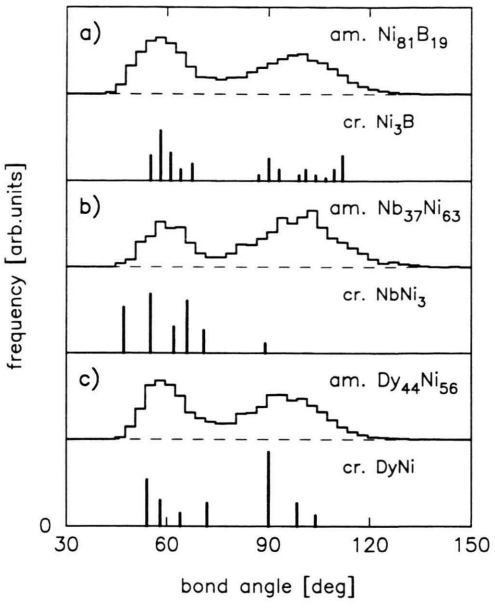


Fig. 9. Amorphous and crystalline A-B alloys: bond angles in triplets of larger atoms (A) which belong to the same coordination shell around a smaller atom (B).

RMC cluster (Figure 9c). It shows the two peak structure, which is typical for metallic glasses, but no distinct preference of the 90° angle, which is characteristic for the square faces of the prisms in crystalline DyNi (see bars in Figure 9c).

In Fig. 9 also the distributions of the bond angle in Ni triplets around B in $Ni_{81}B_{19}$ and in Nb triplets around Ni in $Nb_{37}Ni_{63}$ are plotted. Figure 9 represents a further example of evidence that the similarities between different metallic glasses are much more obvious than the similarities between a certain glass and its individual crystalline counterpart.

The $Dy_{44}Ni_{56}$ metallic glass provides an example to illustrate the important role of the size effect in an attempt to separate the topological and the chemical short range order and to attribute a short range order parameter to the system. Figure 3b shows the Bhatia-Thornton correlation functions $G_{NN}(R)$, $G_{CC}(R)$, and $G_{NC}(R)$ from experiment [4] and from a CR model. The best overall CR fit to the partial $G_{ij}(R)$ in Fig. 3a was obtained with the relative depths 0.8, 1.2, and 1.8 for the Dy-Dy, Ni-Ni, and Dy-Ni potentials and a steeper repulsion for Ni-Ni than for the others. The relative Cargill-Spaepen short range order parameter, $\eta_r = 0.19$, for the model is comparable to the experimental value, $\eta_r = 0.15$ [4]. One, but not the only, possible way to define a statistical reference system, containing the size effect but no chemical effect, is to create an atomic cluster by CR, using the same interaction strength for all pairs as well as additive atomic diameters. The Bhatia-Thornton functions of this statistical reference cluster are included in Figure 3b. Due to the large size effect in the Dy-Ni system the chemical correlation function $G_{CC}(R)$ shows strong oscillations also for the statistical reference system, and it becomes obvious that in such cases the concept of topological and chemical order looses much of its significance. The short range order parameter of this statistical system is not zero, but attains the value $\eta_r = 0.10$.

## 4. General Remarks on the Models

It is acknowledged that, if different atomic configurations can be generated which yield the same pair correlation functions, the Reverse Monte Carlo technique generally creates the most disordered ones, consistent with the experimental data. On the other hand, up to now it is the only type of model yielding agreement which may be classified as perfect (see e.g. the comparison with alternative models for $Ni_{81}B_{19}$ in [14]). The question whether a real glass contains a higher degree of order than the corresponding RMC cluster, such as more regular coordination polyhedra, or whether it presents in fact the most disordered system within the constraints of preferred hetero-coordination and the size effect, can only be answered if alternative models with a higher degree of order than the RMC models will yield comparable agreement. We note that the CR clusters, although involving potentials, did not exhibit more order than the RMC clusters.

In this context it should also be noted that the inhomogeneities in metal-metalloid glasses of size of the order of several tens of Ångstrom units, as observed by small angle scattering, may contain a higher degree of order than the bulk. Their incorporation into a model, if possible at all, will require very large atomic clusters.

## 5. Conclusions

The atomic structure of metallic glasses of different alloy groups is characterized by a chemical short

range order effect and a size effect. The pair potentials are non-additive. Model calculations show that the chemical interaction between the constituents causes preferred hetero-coordination, but does not create specific structural units. Similarities in the topological order of the metallic glasses and of related crystalline phases, if present at all, are confined to atomic distances and coordination numbers. Structural inhomogeneities on larger distance scales, such as phase separation and extended inner surfaces, need further investigation.

[1] P. Lamparter and S. Steeb, Proc. 5th Int. Conf. on Rapidly Quenched Metals, RQ5, North-Holland, Amsterdam 1985, p. 459.
[2] P. Lamparter, W. Sperl, S. Steeb, and J. Blétry, Z. Naturforsch. **37a,** 1223 (1982).
[3] P. Lamparter, M. Schaal, and S. Steeb, Proc. Conf. Neutron and X-ray Scattering: Complementary Techniques, Kent 1989, Inst. Phys. Conf. Ser. No. **101,** 51 (1990).
[4] Ma. Nuding, P. Lamparter, S. Steeb, and R. Bellissent, J. Non-Cryst. Solids, **156–158,** 169 (1993).
[5] P. Lamparter and S. Steeb, 'Structure of Amorphous and Molten Alloys' in: Material Science and Technology, Vol. 1, (VCH, Weinheim 1993), p. 217–288.
[6] S. Steeb and P. Lamparter, J. Non-Cryst. Solids **156–158,** 24 (1993).
[7] P. Lamparter, in: Proc. Euroconference '94 on Neutrons in Disordered Matter, Stockholm, 1994, Phys. Scr. **T75,** 45 (1995).
[8] G. S. Cargill and F. Spaepen, J. Non-Cryst. Solids **43,** 91 (1981).
[9] A. Bhatia and D. E. Thornton, Phys. Rev. B 2, 3004 (1970).
[10] P. Lamparter and S. Steeb, Proc. 4th Int. Conf. on Non-Crystalline Materials, NCM4, J. Non-Cryst. Solids **106,** 137 (1988).
[11] P. Lamparter and B. Boucher, Z. Naturforsch. **48a,** 1086 (1993).
[12] E. H. Brandt and H. Kronmüller, J. Phys. **F17,** 1291 (1987).
[13] R. L. McGreevy and L. Pusztai, Molecular Sim. **1,** 359 (1988).
[14] P. Lamparter, in: Proc. Int. Workshop on Neutron Research and Applications, Budapest, 1994, Acta. Phys. Hung. **75,** 107 (1994).
[15] P. Lamparter, in: Proc. Euroconference '94 on Neutrons in Disordered Matter, Stockholm, 1994, Phys. Scr. **T75,** 72 (1995).
[16] P. H. Gaskell, Nature London **289,** 474 (1981).
[17] J. M. Dubois, P. H. Gaskell, and G. le Caër, Proc. Roy. Soc. London **A 402,** 323 (1985).
[18] P. Lamparter, Z. Naturforsch. **50a,** 329 (1995).
[19] P. Lamparter and S. Steeb, J. Non-Cryst. Solids **192, 193,** 578 (1995).